J. Fluid Mech. (2000), *vol.* 405, *pp.* 131–156. Printed in the United Kingdom

Deformation and breakup of Newtonian and non-Newtonian conducting drops in an electric field

By JONG-WOOK HA AND SEUNG-MAN YANG

Department of Chemical Engineering, Korea Advanced Institute of Science and Technology, Taejon 305-701, Korea

(Received 20 August 1998 and in revised form 7 October 1999)

In this article, we considered experimentally the deformation and breakup of Newtonian and non-Newtonian conducting drops in surrounding fluid subjected to a uniform electric field. First, we examined three distinctive cases of Newtonian-fluid pairs with different relative conductivities, namely highly conducting drops, conducting drops and slightly conducting drops. The results on the Newtonian fluids demonstrated that when the conductivity of the drop is very large relative to that of the surrounding fluid, the deformation response of such highly conducting drops is described well by the electrohydrostatic theory, especially with regard to the prediction of the critical point. Specifically, when the ratio of drop to continuous-phase resistivity, R, was less than 10^{-5}, the electrohydrostatic theory was quite satisfactory. Then, the non-Newtonian effect on the drop deformation and breakup was studied for highly conducting drops which satisfied the condition $R < O(10^{-5})$. The highly conducting drop became stable in a weak or moderate field strength when either the drop or the continuous phase was non-Newtonian. On the other hand, when both the phases were non-Newtonian, more complicated responses were observed depending on the ratio of zero-shear-rate viscosities. Although the effects of the rheological properties are minimal on all features away from the critical conditions for breakup or prior to the instability, the non-Newtonian properties have a significant influence during drop burst, which is accompanied by large velocities and velocity gradients. In particular, when the ratio of the zero-shear-rate viscosity of the drop to that of the ambient fluid was much larger than unity, non-Newtonian properties of the drop phase enhanced the drop stability. Conversely, the elasticity of the continuous phase deteriorated the drop stability. Meanwhile if the zero-shear-rate viscosity ratio was much smaller than unity, the elasticity of the continuous phase produced a stabilizing effect. The effects of resistivity and viscosity ratios on the breakup modes were also investigated. When at least one of the two contiguous phases possessed considerable non-Newtonian properties, tip streaming appeared.

1. Introduction

When a fluid drop is suspended in another immiscible fluid, it can be influenced by an externally applied uniform electric field in many ways. Apart from its basic scientific interest, understanding of the behaviour of drops in an electric field is playing an increasingly important role in practical applications. For example, some of the early studies were motivated by the fact that the drop dynamics in an electric field is of practical significance in birefringence, light scattering, and other

optical measurements of emulsion systems (O'Konski & Thacher 1953; O'Konski & Harris 1957). Part of the interest stemmed also from applications including the deformation and breakup of raindrops in thunderstorms and the breakdown of dielectric liquids due to contaminants such as the water droplets with a substantial conductivity (Sartor 1969; Beard, Ochs & Kubesh 1989). The electric-field-driven flow is of practical significance in the processes in which enhancement of the rate of mass or heat transfer between the drops and their surrounding fluid is desired (Scott 1989; Ptasinski & Kerkhof 1992; Ha & Yang 1999*a*). The problem is also relevant to some aspects of containerless material processing in micro-gravity conditions (Rhim *et al.* 1987; Chung & Trinh 1998). Krause and co-workers reported the use of electric fields to control polymer blend morphology, more specifically the shape and orientation of the dispersed phases (Venugopal, Krause & Wnek 1989; Venugopal & Krause 1992; Xi & Krause 1998; Ha & Yang 1999*b*). More recently, the electrohydrodynamic behaviour of liquid–liquid dispersion systems has been studied rigorously as a new model of electrorheological fluid (Tajiri *et al.* 1997; Pan & McKinley 1997; Ha & Yang 1999*c*). It has been also suggested that the electric field is very effective in biomechanical processes such as cell fission induced in the laboratory with less heat dissipation (Marszalek & Tsong 1995; Winterhalter *et al.* 1996).

There are two simple limits when considering the effect of an external electric field on the drop dynamics. If the two contiguous fluids are considered as perfectly insulating dielectrics and no free charges are present, or if, on the other hand, the drop contains a fluid that is highly conducting while the surrounding fluid is perfectly insulating, an electric field induces a net force at the fluid interface as a result of discontinuity in the electric stresses (Melcher & Taylor 1969). Because this electric surface force acts only in the direction normal to the interface, it can be balanced by the interfacial tension. Therefore, the drop is always elongated into a prolate shape with its axis of symmetry parallel to the direction of the applied field, while the fluids remain motionless at a steady state. These ideal situations of electrified drops have been extensively studied within the well-established theoretical framework of *electrohydrostatics* (for example, O'Konski & Thacher 1953; Garton & Krasucki 1964; Taylor 1964; Miksis 1981; Basaran & Scriven 1989; Basaran & Wohlhuter 1992; Wohlhuter & Basaran 1992; Stone, Lister & Brenner 1999).

When finite conductivity of fluid is considered, the problem becomes more interesting yet complicated. One of the most noteworthy phenomena is that, in addition to the prolate shape predicted by the electrohydrostatic theory, a drop in an electric field may remain in a spherical shape or even be deformed into an oblate spheroid as observed in experiments (Allan & Mason 1962; Torza, Cox & Mason 1971; Arp, Foister & Mason 1980; Vizika & Saville 1992; Ha & Yang 1995). Taylor (1966) recognized that finite conductivity enables electrical charge to accumulate at the drop interface, permitting a tangential electric stress to be generated. The tangential electric stress drags fluid into motion, and thereby generates hydrodynamic stress at the drop interface. The complicated interplay between the electric and hydrodynamic stresses causes either oblate or prolate drop deformation, and in some special cases keeps the drop from deforming. This *electrohydrodynamic* theory proposed by Taylor is referred to as the leaky dielectric model, and is capable of predicting the drop deformation in qualitative agreement with the previous experimental observations.

Although Taylor's leaky dielectric theory provides a good qualitative description for the deformation of a Newtonian drop in an electric field, the validity of its analytical results is strictly limited to the drop experiencing small deformation in an infinitely extended domain. Extensive experiments conducted by Torza *et al.* (1971) showed

a serious quantitative discrepancy with Taylor's theoretical prediction. Drops were found to be consistently more deformed than would be expected from the theoretical prediction. Furthermore, when the drop phase is less conducting than the ambient fluid, the less conducting drop executes so-called electrorotation even in a uniform electric field (Ha & Yang 1999*d*). To resolve the quantitative discrepancy between theory and experiment, Ajayi (1978) extended the linearized asymptotic model of Taylor to include higher-order corrections for the nonlinear terms. Although Ajayi's asymptotic theory predicted the drop deformation more accurately, the higher-order corrections were found to be insufficient to remove fully the discrepancy. To examine electrokinetic effects, the leaky dielectric model was replaced by a model which considered the charge transport (Baygents & Saville 1989; Saville 1997; Feng 1999). Even though the microscale motions and diffused charge layers were more accurately described, the calculated drop deformation turned out to be exactly the same as that given by the leaky dielectric model. Thus, the leaky dielectric model is accepted as a correct lumped-parameter model when no net charge exists on the drop. Since none of the obvious theoretical extensions seemed to be able to resolve the serious discrepancy, Vizika & Saville (1992) performed a rigorous experimental investigation. Although certain discrepancies remained for some cases, their results appeared to agree with the asymptotic leaky dielectric prediction better than the previous experiments.

While the asymptotic leaky dielectric theory gives a satisfactory description for the behaviour of a conducting Newtonian drop in an insulating medium within the small deformation limit, the electrohydrostatic theory predicts more readily the critical electric field strength above which the drop loses its stable configuration. It has been shown that Taylor's (1964) spheroidal approximation is in good agreement with more rigorous numerical methods if the drop is perfectly conducting. Recently, Feng & Scott (1996) reported a computational analysis for the deformation and stability of a leaky dielectric drop in a uniform electric field. Although agreement between the experimental results and the theory improved considerably, their result reduced to Taylor's when the drop was perfectly conducting.

Although Newtonian fluids are ubiquitous in practical applications, non-Newtonian fluids also appear in myriad important applications. These fluids contain high-molecular-weight polymers and are characterized by nonlinear stress–strain relationships, elasticity, and finite time scales for stress relaxation. Unlike the Newtonian fluids, there are few available theoretical investigations which pertain to the deformation and stability of the interface between the non-Newtonian fluids in an electric field. This is mostly because of the anticipated uncertainties in selecting an appropriate constitutive model for non-Newtonian fluids, as well as the obvious difficulty in solving the equations of motion after the choice has been made. Instead, in the present study, we consider experimentally the effect of non-Newtonian properties on the drop deformation and breakup, and identify the role of the non-Newtonian response by comparing the deviations from the well-known theories or experimental observations for a Newtonian-fluid pair.

In the remainder of this paper, we report a series of experiments to elucidate the effect of non-Newtonian properties of the constituent fluids on the drop deformation and breakup in an electric field. The main objective of our study on non-Newtonian polymeric drops is to elucidate the effect of non-Newtonian properties on the critical point above which the drop loses its stable configuration. If we have a reliable theory that accounts for the elastic or viscoelastic nature of fluids successfully, the experimentally observed non-Newtonian responses may be explained based on the theory. Unfortunately, this approach cannot be easily accomplished due to the fact

that the systematic theoretical interpretation of non-Newtonian properties of the fluids is extremely difficult. Another approach is purely experimental, that is, a direct comparison of non-Newtonian drops with Newtonian drops possessing exactly the same electrical and viscometric properties except for some elastic or viscoelastic characteristics. This is also difficult to achieve because we cannot control each fluid property independently. While a lot of theoretical works on Newtonian drops are available in literature, especially for the critical point of perfectly conducting drops for which *electrohydrostatic* theory is applicable, the validity of the critical point predicted from the electrohydrostatic theory has not been yet completely proved for a wide range of electrical properties of fluids. In the present study, we determine the range of the resistivity ratio R within which the electrohydrostatic theory is valid for the Newtonian-fluid pair, especially for the prediction of the critical point. Then, we consider the responses of highly conducting non-Newtonian drops for which electrohydrostatics is valid. In this case, the deviation from Newtonian fluid behaviour can be regarded as a consequence of non-Newtonian characteristics. As we shall see shortly, the non-Newtonian effect on the drop dynamics is successfully identified on the basis of electrohydrostatics at least qualitatively. In addition, we clearly observe deformation and breakup modes of the non-Newtonian drops which are distinctively different from the Newtonian cases.

2. Experimental

2.1. *Apparatus and procedures*

The experimental apparatus and the procedures were identical to those of our previous study (Ha & Yang 1998). The drop phase was formed by dispensing an exact volume of fluid by an accurate micropipette. The typical volume of the initially undeformed drop was 10 μl, or equivalently 0.134 cm in radius. Since the densities of the two contiguous phases were matched, buoyancy effects were excluded.

After the drop was placed in the middle of the two copper-plate electrodes, the electric field was applied by a high-voltage power supply (Glassman High Voltage Inc., Series EH). A CCD camera (Watec Inc., Wat-201) equipped with microscopic lenses was used to take images of the deformed drop shape, which were recorded by a VCR and captured by a frame grabbing board, if necessary. The degree of deformation at a given electric field strength was calculated from the captured images. The degree of drop deformation can be expressed conveniently by the parameter defined by

$$D = \frac{(L - B)}{(L + B)}, \tag{2.1}$$

in which L and B are the drop lengths parallel and perpendicular to the electric field, respectively. This parameter is especially sensitive to small deviations from sphericity. In the present experimental study, none of the *steady-state* drop shapes were highly elongated and D was used exclusively to define the deformed drop shapes. After determining the critical electric field strength above which no steady-state shape of drop existed, the drop breakup modes were studied. The time-dependent deformation of the drop was continuously recorded through the CCD camera at slightly higher electric field strength than its critical value.

2.2. *Measurement of material properties*

The electrical properties of the fluids in this study were measured by a similar method to that reported by Vizika & Saville (1992) for the measurement of dielectric

constants. Two copper electrodes of 5 cm in radius were separated by a 0.1 cm gap. With this cell, the dielectric constants were calculated from the measured capacitance. The contribution from the empty cell was considered using standard materials such as hexane, glycerol, and ethyl alcohol. Since one of the objectives of this study is to find the condition for validity of the electrohydrostatic theory, the conductivities of the fluids and their dependence on the electric field strength are important. Ordinary conductivity meters were not appropriate for leaky dielectric materials such as silicone oil and polybutene solutions used as an insulating continuous phase. A very high voltage was required when the cell was filled with a low-conductivity fluid and the current through the circuit could be measured only by a sensitive ammeter (Yokogawa Electric Corp., Model 2011). Through the voltage–current relationship, the fluid conductivity was estimated. Obviously, this method does not provide the exact value of the fluid conductivity, but gives sufficient information since the relative magnitude of the electrical properties between the drop and the continuous phases is much more important rather than their individual values.

The rheological properties of the fluids used here were measured by ARES fluid rheometer (Rheometric Scientific Inc.). The viscosities were measured for shear rates ranging from $0.1\,s^{-1}$ to $100\,s^{-1}$. The elastic nature of non-Newtonian polymeric fluids was interpreted usually via the normal stress difference. One of the difficulties involved in the study of non-Newtonian fluids arises from the fact that the viscosity μ is not a unique quantity (Bird, Armstrong & Hassager 1987). Specifically, the shear viscosity differs from the extensional viscosity, both of which are usually influenced by the rate of deformation. Therefore, the shear viscosity of a fully viscoelastic fluid exhibits shear-thinning behaviour. Herein, we defined the viscosity ratio λ in terms of the steady shear viscosity instead of the extensional viscosity. For the shear-thinning fluids, we defined the ratio of the viscosity, λ, of the drop phase to that of the ambient fluid in terms of the zero-shear-rate viscosities exclusively. As we shall see later, the neglect of shear dependence of the viscosity does not oversimplify the problem, especially for the conducting drops, since the electric-field-induced flow is too weak to induce an appreciable rheological effect. Under these circumstances, the role of non-Newtonian effects arises from the fluid elasticity. This is especially true when the field strength is below its critical value or prior to the instability.

The determination of the interfacial tension, γ, is not easy because the fluids used in this study are very viscous and have almost the same densities. Therefore, conventional techniques for interfacial tension measurements such as the pendant drop, ring or plate methods are not appropriate. One simple way to estimate the interfacial tension is based on the small deformation theory describing the relationship between the degrees of drop deformation and electric field strength (Taylor 1966), i.e.

$$D = \frac{9}{16(2R+1)^2}\left[(1+R^2-2SR^2)+3R(1-SR)\frac{2+3\lambda}{5+5\lambda}\right]\frac{a\epsilon E^2}{\gamma}, \tag{2.2}$$

where R, S and λ denote the ratios of resistivity, permittivity and viscosity of the drop to those of the continuous phase, respectively. In addition, a is the radius of the initially spherical drop, ϵ is the permittivity of the continuous phase and finally, E is the electric field strength. Thus, Taylor's theory for the drop deformation in a weak electric field may offer a convenient measure of the interfacial tension. In the present study, Taylor's small deformation theory was used to obtain the interfacial tension. Therefore, as we shall see shortly, the experimental deformation data and theory coincide at small deformations. The dimensionless group, $a\epsilon E^2/\gamma$ is sometimes

referred to as the dimensionless electric field strength or the electric capillary number†, ($\mathscr{C}$), due to the analogy with the capillary number, $\mu u_c/\gamma$, which is frequently used in studies of drop dynamics under external flow fields in the low Reynolds number limit. In fact, the characteristic velocity u_c is given by $a\epsilon E^2/\mu$ for electrohydrodynamic flow.

Meanwhile, although Taylor's theory is valid strictly for the case of Newtonian fluids, it is not applicable in general when at least one of the fluids is viscoelastic. However, the first correction to Taylor's theory taking into account the viscoelastic effects occurs at the order of Deborah number. In the small deformation limit, therefore, the viscoelastic correction is expected to be small because the electric-field-driven flow is very weak at modest electric field strength.

3. Deformation and breakup of Newtonian drops suspended in Newtonian fluid

3.1. *Materials*

In the present section, we consider the deformation and breakup of Newtonian fluid drops suspended in another Newtonian fluid in a uniform electric field. The primary objective of this section is twofold: first, to determine the range of resistivity ratios R within which the electrohydrostatic theory is applicable, and then to examine the effect of viscosity ratio λ or resistivity ratio R on the breakup modes. The Newtonian results are expected to provide a basis on which the breakup behaviour of elastic or viscoelastic fluid drops can be considered.

To elucidate the effect of viscosity ratio, silicone oils of various viscosity grades were prepared. Silicone oils B, C, and E were obtained by mixing highly viscous silicone oil (KF-96, 10000 cS) with a less viscous one (KF-96, 50 cS) both purchased from Shin-Etsu Silicone. Other properties of silicone oil apart from viscosity were not changed appreciably. To examine the effect of the ratio R of drop to continuous-phase resistivity, we prepared three types of fluid samples, namely highly conducting fluids ($R < 10^{-5}$), conducting fluids ($R \sim 10^{-4}$) and slightly conducting fluids ($R \sim 10^{-1}$). Table 1 contains the experimental runs and relevant parameters for each experimental system. For highly conducting drops, we prepared deionized water (W1), an aqueous solution of potassium chloride (W2), and a mixture of water, ethyl alcohol and dissolved polyvinylpyrrolidone (N1). As a second class of conducting fluid, a mixture of glycerine–ethyl alcohol (N2) and glycerine–propanol (N3) was prepared. In addition, three polymeric Newtonian solutions (N3A, N3B, N3C) were formed by dissolving 3, 7, 15 wt% of polyvinylpyrrolidone in a glycerine–propanol mixture, respectively. Although polymeric in nature, the polyvinylpyrrolidone (PVP) solutions behave as a Newtonian fluid over the shear-rate ranges of viscosity measurement. Finally, we chose castor oil as an example of a leaky dielectric drop possessing slightly higher or comparable conductivity relative to that of the ambient fluid.

3.2. *Deformation and breakup of Newtonian drops*

Let us then begin by considering the deformation and stability of a drop which is highly conducting compared with the suspending fluid. In figure 1(*a*), the degree of deformation D is plotted versus the electric capillary number, $\mathscr{C}$, for the case of both

† Sometimes, the dimensionless group has been referred to as the electrical Weber number. As one of the referees indicated, the Weber number may be an inappropriate definition in this problem where the inertial force is not important. On the other hand, as employed by others (Kang 1993; Cho *et al.* 1996), the electrical Weber number is probably correct when the inertia is significant.

System	Drop phase	Continuous phase	R	S	λ	Interfacial tension ($\mathrm{N\,m^{-1}}$)
NN1	W2	SD	$< 10^{-8}$	31.1	0.001	0.0310
NN2	W1	SD	$< 10^{-6}$	28.2	0.001	0.0284
NN3	N1	SA	$< 10^{-5}$	19.8	0.004	0.0058
NN4	N1	SB	$< 10^{-5}$	19.8	0.006	0.0059
NN5	N1	SC	$< 10^{-5}$	19.8	0.014	0.0058
NN6	N1	SD	$< 10^{-5}$	19.8	0.043	0.0054
NN7	N1	SE	$< 10^{-5}$	19.8	0.006	0.0053
NN8	N2	SA	$\sim 10^{-4}$	12.9	0.016	0.0040
NN9	N2	SB	$\sim 10^{-4}$	12.9	0.022	0.0039
NN10	N2	SC	$\sim 10^{-4}$	12.9	0.053	0.0040
NN11	N2	SD	$\sim 10^{-4}$	12.9	0.160	0.0037
NN12	N2	SE	$\sim 10^{-4}$	12.9	0.175	0.0038
NN13	N3	SD	$\sim 10^{-4}$	12.9	0.050	0.0025
NN14	N3A	SD	$\sim 10^{-4}$	13.7	0.083	0.0027
NN15	N3B	SD	$\sim 10^{-4}$	13.7	0.175	0.0029
NN16	N3C	SD	$\sim 10^{-4}$	14.0	0.542	0.0036
NN17	CO	SA	~ 0.1	1.37	0.080	0.0040
NN18	CO	SB	~ 0.1	1.37	0.111	0.0037
NN19	CO	SC	~ 0.1	1.37	0.266	0.0038
NN20	CO	SD	~ 0.1	1.37	0.800	0.0034
NN21	CO	SE	~ 0.1	1.37	0.874	0.0033

TABLE 1. The list of experimental runs for the deformation and breakup of Newtonian drops suspended in another Newtonian fluid. (W1: deionized water, W2: 0.1 M KCl aqueous solution, N1: 1 wt% polyvinylpyrrolidone solution in water–ethanol mixture, N2: glycerine–ethanol mixture, N3: glycerine–propanol mixture, N3A, N3B, N3C: 3, 7, 15 wt% polyvinylpyrrolidone solution in N3, CO: castor oil, SA: silicone oil A, $\mu = 9.80$ Pa s, SB: silicone oil B, $\mu = 7.04$ Pa s, SC: silicone oil C, $\mu = 2.95$ Pa s, SD: silicone oil D, $\mu = 0.98$ Pa s, SE: silicone oil E, $\mu = 0.90$ Pa s)

a water drop (W1) and a drop of *very highly* conducting aqueous potassium chloride solution (W2) dispersed in silicone oil D. In this case, the resistivity ratio $R < O(10^{-6})$ and thus this is the case of highly conducting drops in an almost insulating medium. Also included for comparison is a deformation curve of Feng & Scott (1996) for a perfectly conducting drop calculated from the electrohydrostatic theory until the steady-state shape no longer exists. Thus, the largest electric capillary number for the deformation curve in figure 1(*a*) corresponds to the critical electric capillary number for the existence of a steady-state solution. The experimental data represented by various symbols are also collected until the steady-state shape disappears. The asterisk which appears in the figure represents the critical capillary number, $\mathscr{C}_c$, estimated from the $O(\mathscr{C}^2)$ asymptotic solution for the drop shape (Ha 1999). As noted from figure 1(*a*), both the numerical and asymptotic analytical results agree well with the experimental results, especially when the degree of deformation is quite small. However, as the drop deforms further, a slight discrepancy between theory and experiment appears. The linearized asymptotic solution underestimates the degree of deformation whereas the numerical prediction slightly overestimates it. Many investigators have reported the critical electric capillary numbers for a perfectly conducting drop; some are summarized in table 2. The critical electric capillary numbers predicted by various methods are in good agreement with the experimental observation in this case.

In figure 1(*b*), the degree of deformation is plotted for another highly conducting drop, polyvinylpyrrolidone dissolved in water–ethyl alcohol (N1) dispersed in various

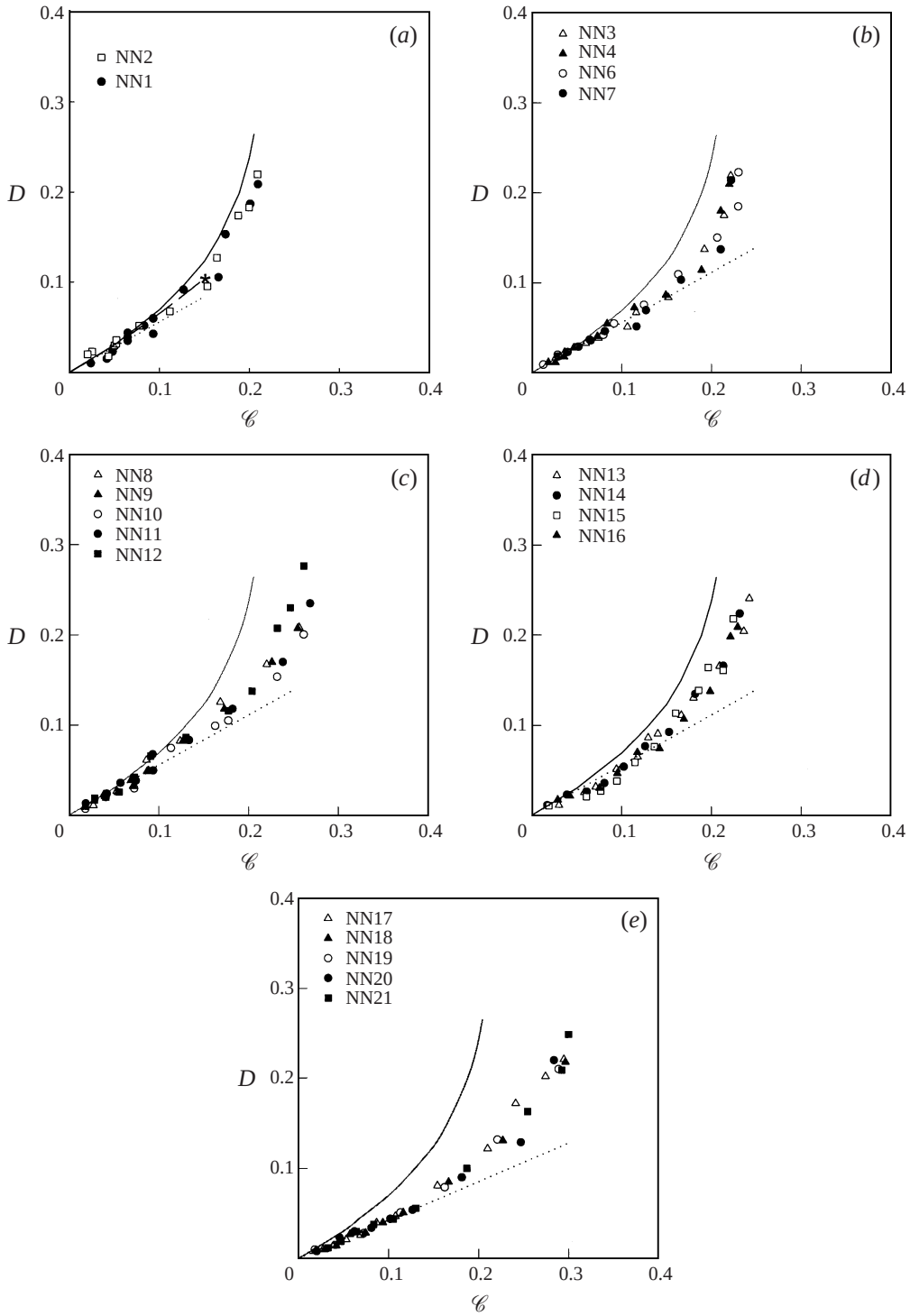

FIGURE 1. For caption see facing page.

Methodology	$\mathscr{C}_c$	D_c
Minimum energy principle	0.205	0.289
Taylor (1964, spheroidal approximation)	0.210	0.310
Miksis (1981, numerical method)	0.209	0.293
Sherwood (1988, boundary-integral method)	0.206	0.259
Basaran & Scriven (1989, FEM)	0.207	0.291
Feng & Scott (1996, FEM)	0.210	0.270
$O(\mathscr{C}^2)$ asymptotic solution	0.147	0.109
Experiments	0.214	0.220

TABLE 2. The camparison of published critical capillary number ($\mathscr{C}_c$) and corresponding degree of drop deformation (D_c) for perfectly conducting drop. Experimentally determined values are averages of experiments NN1 to NN7.

silicone oils. The deformation curves of N1 drops determined by experiments are slightly different from those shown in figure 1(*a*). This is because the conductivity of drop N1 is lower than those in figure 1(*a*), i.e. in this case, $R \sim O(10^{-5})$. However, the electrohydrostatic theory of Feng & Scott (1996) for a perfectly conducting drop still provides a fairly good approximation to the drop deformation. When the drop conductivity decreases further, the deviation is expected to be greater. In figures 1(*c*) and 1(*d*), the deformation curves are plotted for $R \sim O(10^{-4})$. Indeed, as seen from figure 1(*c*), experimental results for conducting drops of glycerine–ethanol mixture (N2) immersed in silicone oils deviate significantly from those for a perfectly conducting drop although the drops can be still considered conducting. In this case, the critical electric capillary numbers of conducting drops are higher than those of highly conducting drops and the numerical electrohydrostatic solution underestimates the critical value significantly. Meanwhile, as noted from figure 1(*d*), the deformation behaviour of conducting drops either of a glycerine–propanol mixture (N3) or of polyvinylpyrrolidone solution in N3 (N3A, N3B, and N3C) deviates slightly from the deformation response of the highly conducting drops in figure 1(*b*). In this case, the critical capillary number predicted from the numerical simulation of Feng & Scott (1996) is slightly lower than the experimental value. Thus, although the drop deformation is strongly influenced by the resistivity ratio R, the difference between $R \sim O(10^{-5})$ and $R \sim O(10^{-4})$ is not sufficiently large to override the effects arising from the other electrical and interfacial properties. It is noteworthy that when the drop is conducting or highly conducting, i.e. when $R < O(10^{-4})$, the electric-field-driven flow is very weak, especially prior to the drop burst. Consequently, the experimental results show that the viscosity ratio is not an important parameter because its effect on the drop deformation is very small in this weak flow. The relative deviations of the experimen-

FIGURE 1. Degree of deformation a drop as a function of the electric capillary number $\mathscr{C}$ in the case of a conducting drop. (*a*) Drops of deionized water and KCl aqueous solution in silicone oil (the dashed line is the $O(\mathscr{C}^2)$ theory and the asterisk represents the critical capillary number estimated from linear stability analysis); (*b*) drops of PVP dissolved in water–ethyl alcohol mixture (N2) in silicone oils; (*c*) drops of glycerine–ethyl alcohol mixture (N2) in silicone oils; (*d*) drops of glycerine–propanol mixture (N3) and Newtonian PVP (N3A, N3B, N3C) in silicone oil D; (*e*) castor oil drops in silicone oils. The solid lines are the computational curves of Feng & Scott (1996) from the electrostatic theory for a perfectly conducting drop; the dotted lines are the first-order asymptotic leaky dielectric theory of Taylor. Details are given in table 1.

tal critical capillary numbers for conducting drops are within 20% of the theoretical prediction of $\mathscr{C}_c = 0.210$ for a perfectly conducting drop (Feng & Scott 1996).

Let us now consider the deformation and breakup of a drop with conductivity comparable to the continuous phase. In figure 1(*e*), the deformation curve is plotted for $R \sim O(10^{-1})$. In this case, unfortunately, numerical solutions which exactly reflect our experimental conditions are not available. Thus, we included again here the numerical deformation curve for a perfectly conducting drop to examine the degree of deviation from the case for a slightly conducting drop. Also shown for illustration is the asymptotic curve from leaky dielectric theory. As expected, the numerical solution for a perfectly conducting drop deviates significantly from the experimental results for a slightly conducting drop even at small deformations.

For a highly conducting drop, the electric-field-driven flow is sufficiently weak that the total energy of the system comes mainly from the interfacial and electrical contributions. In this case, the degree of deformation at a given capillary number is determined from the condition of minimum total energy at equilibrium considering only the electrical and interfacial contributions. Thus, the behaviour of a highly conducting drop can be well described by a single master deformation curve, which is expressed in terms of the degree of deformation versus $\mathscr{C}$. In general, the critical electric capillary number depends on the resistivity ratio (R) and is a weak function of both the viscosity ratio (λ) and the permittivity ratio (S). It is known, at least numerically, that a generic electrohydrostatic assumption with no fluid motions is satisfactory when $R < 10^{-5}$. This agrees well with the present experimental results. Linear stability analysis based on the $O(\mathscr{C}^2)$ small deformation theory shows that the critical capillary number increases as R becomes larger than $R \sim 10^{-3}$, below which it remains nearly constant (Ha 1999). The increase in R improves the drop stability, which is also consistent with the experiments.

Although a number of experimental works concerning the deformation and breakup of a Newtonian drop in a uniform electric field are available in literature, the full deformation curve predicted from theory has not been tested yet. Comprehensive and careful experiments were carried out by Torza *et al.* (1971) and Vizika & Saville (1992), but they only confirmed the validity of theory within the small deformation limit (approximately, $D < 0.1$ and $\mathscr{C} < 0.15$). On the other hand, Moriya, Adachi & Kotaka (1986) considered the behaviour of drops far beyond the small deformation limit until the burst of the drop could be observed. In spite of the fact that some of the fluids employed were highly concentrated polymeric solutions, the authors did not pay any attention to the non-Newtonian characteristics. Previously, we have confirmed that the behaviour of a highly conducting drop in an insulating medium could be fairly well described by the theory for a perfectly conducting drop (Ha & Yang 1998, 1999*b*). In the present work, we provide more reliable evidence about the range of validity of the electrohydrostatic theory by considering a wide range of the fluid properties.

In fact, our experimental results seemed to agree perfectly with the small deformation theory, while the results of Torza *et al.* and Vizika & Saville deviated from theory considerably in some systems. However, this does not imply that their results are incorrect. Torza *et al.* and Vizika & Saville determined interfacial tensions by independent static means rather than by small deformation theory. The discrepancy of their results may arise from the interfacial tensions they used. In this study, however, the interfacial tension was determined from the small deformation theory as an adjustable parameter. Furthermore, in the plots of Torza *et al.* and Vizika & Saville, the degree of drop deformation was expressed as a function of aE^2. By doing this,

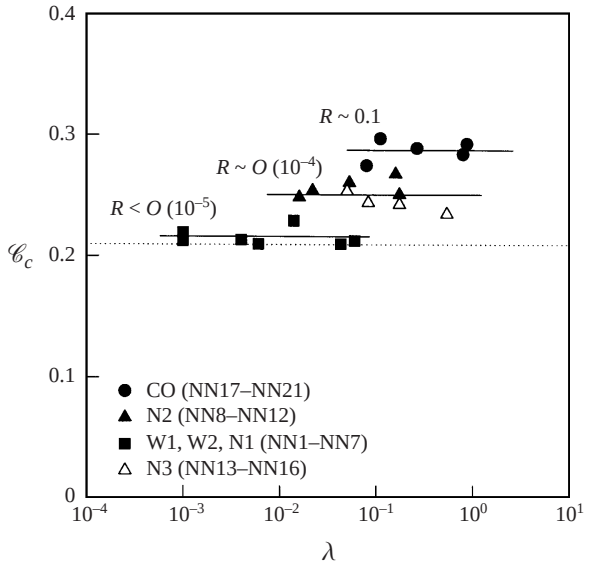

FIGURE 2. Critical capillary numbers, $\mathscr{C}_c$, for each system (see table 1) as a function of the viscosity ratio λ. The dotted line is the perfectly conducting limit predicted by Feng & Scott (1996) from the numerical simulations.

a slight difference in the value of interfacial tensions produced a deviation from theory even in the small deformation limit although the data set preserved linearity. In contrast, since we obtained the interfacial tensions from the linear theory, our data sets agreed with the theory exactly in the small deformation limit. Selected data sets of Vizika & Saville for highly conducting drops were plotted again by Feng & Scott (1996) as a function of the dimensionless quantity which was equivalent to the electric capillary number used here. In this plot, the data sets were coincident with the theory very accurately within the small deformation limit of $D < 0.05$. In this region, both the leaky dielectric theory and the numerical calculation provided an excellent prediction. The present results contained in figures 1(*b*)–1(*e*) showed that the deformation behaviour of a conducting or slightly conducting drop deviated considerably from the linear theory or numerical calculations for a perfectly conducting drop. This was because the drop fluids did not behave like a perfectly conducting fluid. Thus, the electrohydrostatic theory fails to predict the deformation behaviour of a conducting or slightly conducting drop. In this case, the electric-field-induced flow is appreciable compared to the case of a highly conducting drop.

In figure 2, the critical electric capillary numbers measured from the present experiments are summarized. The dotted line corresponds to a perfectly conducting drop. As mentioned earlier, the critical capillary numbers are nearly independent of the viscosity ratio and increase when the resistivity ratio R approaches unity. It can be also noted again from figure 2 that the electrohydrostatic theory is valid when the resistivity ratio R is smaller than 10^{-5}.

3.3. *Breakup modes of Newtonian drops*

In figures 3–7, typical images of bursting Newtonian drops are reproduced. The first breakup mode shown in figure 3 was usually observed in the case of highly conducting drops such as deionized water or potassium chloride aqueous solution. As seen, a highly conducting water drop in silicone oil A ($R < 10^{-6}$) is initially elongated into an

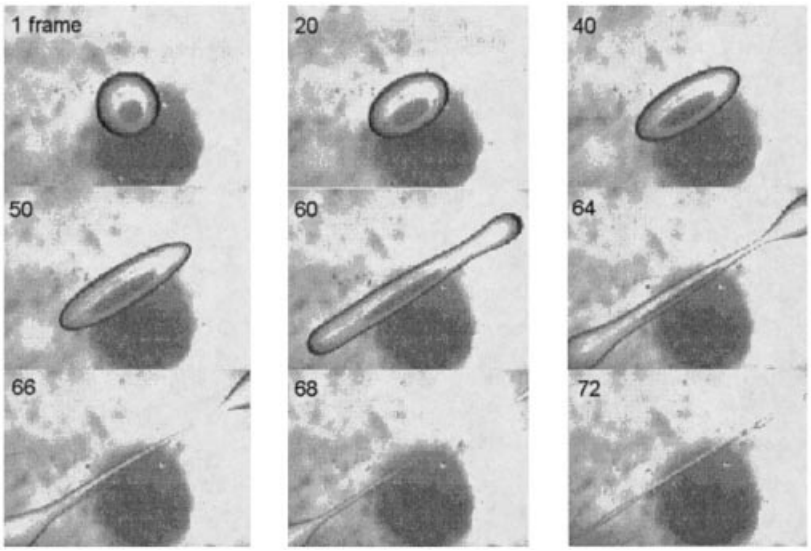

FIGURE 3. Breakup of a water drop in silicone oil A (system NN2 in table 1). The radius of the initial spherical drop is 0.25 cm and the applied electric field strength is 3.2 kV cm^{-1} ($\mathscr{E} = 1.1\mathscr{E}_c$). The frame rate is 15 frames s^{-1}.

ellipsoidal shape until it forms a rod with rounded ends (frames 1–50). About 4 s after the electric field has been changed, a single pinching region is developed in the rod section of the drop (frame 60). Shortly after the development of a pinching region, the drop deformation suddenly starts to increase rapidly, and the bulbous ends split into two main parts joined by a thread (frames 60–68). Subsequently, the thread breaks into a number of small drops (frame 72). Consequently, a highly conducting water drop in silicone oil A is fractured into two relatively large daughter drops and several tiny satellite drops. This type of breakup in an electric field has been reported frequently for highly conducting drops: for instance, a water–sextol phthalate system (Allan & Mason 1962), water–castor oil system (Torza *et al.* 1971) and water–silicone oil system (Ha & Yang 1998). In figure 4, electric burst is illustrated by the cinematographs for another highly conducting drop, N1 in silicone oil D. In this case, the resistivity ratio R is less than 10^{-5}. Although the N1 drop possesses slightly lower conductivity than the water drop considered in figure 3, the general features of drop breakup are changed significantly. In the initial stage, the N1 drop deforms into an elongated ellipsoid, similarly to the water drop. It can be readily seen, however, that the N1 drop deforms very slowly compared to the water drop until it reaches a certain degree of deformation (frame 139). Immediately after reaching the critical deformation, the drop begins to stretch rapidly, but the ends bulb suddenly and the development of a pinching region near each bulbous end is evident (frame 140). Then, the blob at each end moves further away and the constricted regions become narrower, thereby forming a neck that joins the main body. As time proceeds, the neck pinches and eventually breaks into a few small satellite drops leaving two daughter drops at the ends and a large main body in the mid-part (frame 142). Therefore, the end-pinching mechanism leads to drop breakup.

Now let us then consider the electric-field-induced burst of a conducting N3 drop in silicone oil D for which $R \sim 10^{-4}$. As noted from figure 5, the droplet also fragments according to the end-pinching mechanism (frames 510 and 550). However, after the

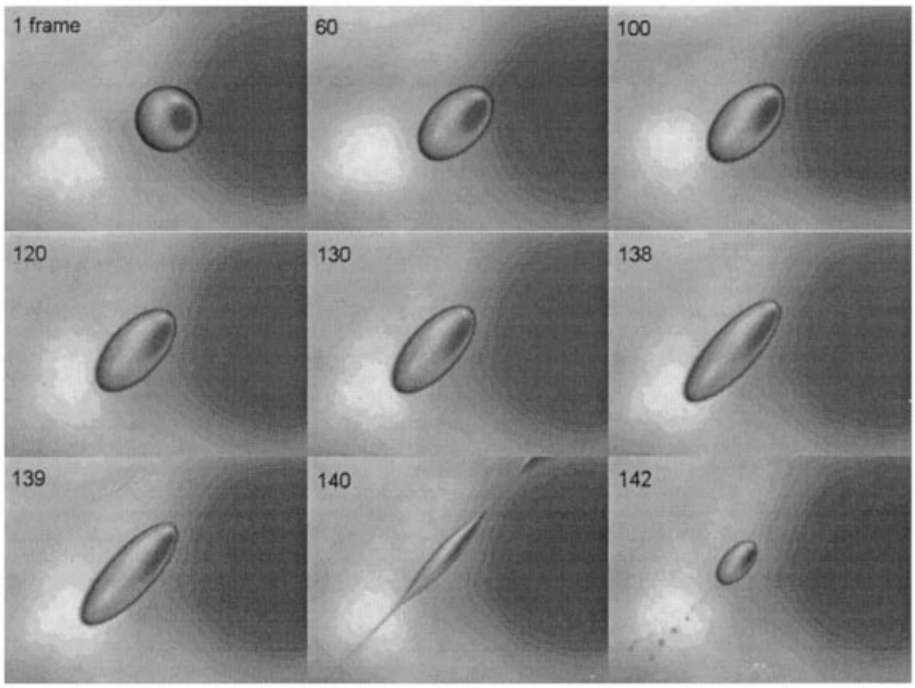

FIGURE 4. Breakup of an N1 drop (PVP dissolved in water–ethyl alcohol mixture) in silicone oil D (NN6 in table 1). The radius of the initial spherical drop is 0.14 cm and the applied electric field strength is 4.5 kV cm^{-1} ($\mathscr{E} = 1.2\mathscr{E}_c$). The frame rate is 15 frames s^{-1}.

first pinch-off, in this case, the main mid-part stretches into a thin thread rather than relaxes into an ellipsoid like the highly conducting N1 drop considered in figure 4. Then, the thin thread in the mid-part fragments into a few small droplets due to the capillary instability (frames 730–850). Electric-field-induced breakup of the slightly conducting castor oil drops in silicone oils is displayed in figures 6 and 7. In this case, the resistivity ratio $R \sim 0.1$. As noted, the global burst features of the slightly conducting drops are similar to those of the conducting N3 drop. It is also noted from figures 5–7 that the size of the two bulbous ends decreases and a larger fraction of the drop remains in the main mid-part as the conductivity of the drop phase is reduced. After the two ends tear off, the remainder of the drop is elongated continuously and eventually broken up into several drops, similarly to the breakup of a highly extended thin liquid thread.

As previously mentioned, the general features of the drop deformation are not significantly influenced by the viscosity ratio prior to the drop burst, see figure 1(*e*). However, the viscosity ratio is an important parameter in the mode of the drop breakup. This is because the fluid motions inside and outside a slightly conducting drop become relatively significant, when the electric field is strong enough to induce drop breakup. The role of viscosity ratio in the drop breakup mode can be seen from comparing figures 6 and 7, which correspond to the viscosity ratio $\lambda = 0.080$ and 0.874, respectively. The initial stage of drop breakup looks similar, independently of the viscosity ratio. For the less viscous drops (NN17), the breakup mode was nearly the same as in figure 5. In contrast, for a fluid pair with comparable viscosities, the breakup proceeded differently: for example, a castor oil drop in comparably viscous silicone oil (i.e. NN20 and NN21) showed a breakup mode different from the case

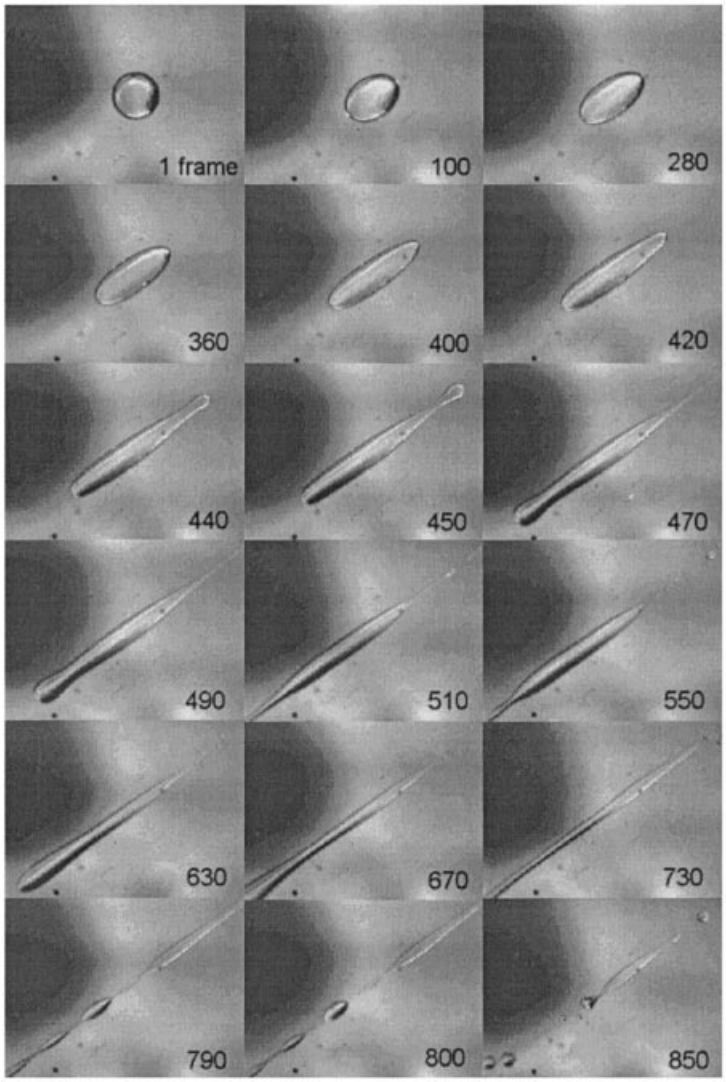

FIGURE 5. Breakup of an N3 drop (glycerine–propanol mixture) in silicone oil D (NN13 in table 1). The radius of the initial spherical drop is 0.11 cm and the applied electric field strength is 3.1 kV cm^{-1} ($\mathscr{E} = 1.1\mathscr{E}_c$). The frame rate is 14 frames s^{-1}.

of castor oil drop in highly viscous silicone oil. As shown in figure 7 for NN21, the castor oil drop elongated into a thin thread with sharply pointed ends in a comparably viscous medium. Several pinching necks (or waists) were also formed. Although the drop ends become pointed, we do not refer this mode to tip streaming. Tip steaming is usually defined as a breakup mode of a drop possessing ellipsoidal shape with pointed ends during the breakup process, as we shall see in the next section. A similar phenomenon was observed for the more conducting drops of PVP solution dissolved in glycerine–propanol mixture (NN16) with conductivities about a thousand times as large as castor oil.

For highly conducting drops, Torza *et al.* called the breakup 'electric burst' since there was no appreciable electrohydrodynamic flow inside and outside the drop. In this case, the breakup occurs when the interfacial tension can no longer support the normal

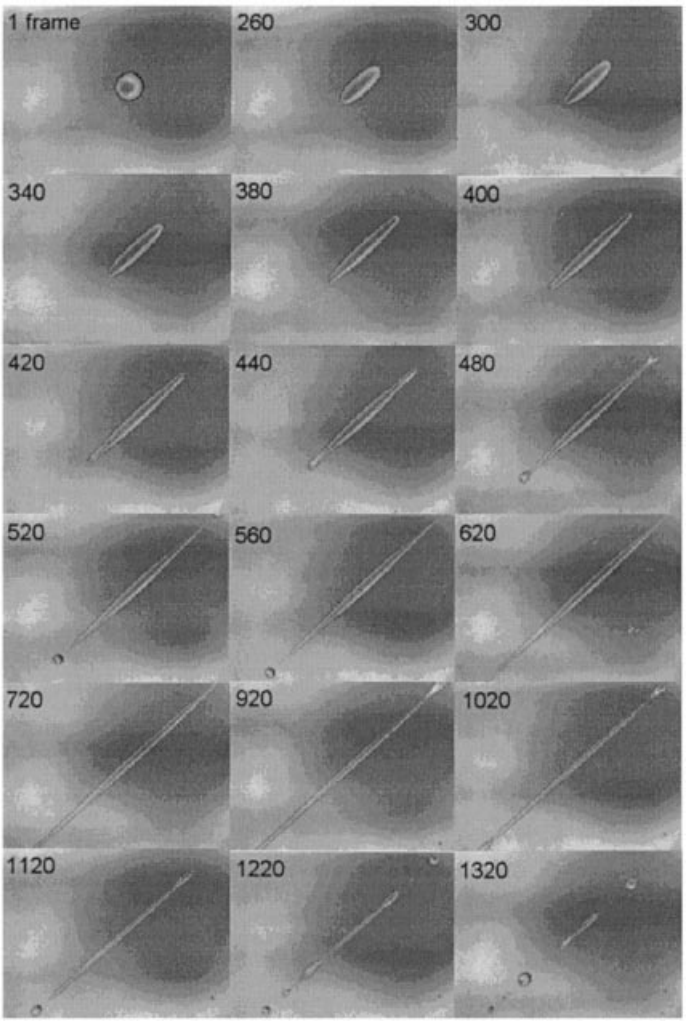

FIGURE 6. Breakup of a castor oil drop in silicone oil A (NN17 in table 1). The radius of the initial spherical drop is 0.13 cm and the applied electric field strength is 3.7 kV cm^{-1} ($\mathscr{E} = 1.2\mathscr{E}_c$). The frame rate is 15 frames s^{-1}.

electric stress. While many computational results for predicting the critical capillary number are available, numerical simulations of the shape evolution in the course of breakup are relatively limited. Using a boundary integral method, Sherwood (1988) examined the deformation of a drop over a wide range of permittivity and conductivity ratios but with the viscosity ratio fixed at unity. It is suggested that there are two modes of breakup: pointed end formation when the ratio S of the permittivity of the drop phase to that of the surrounding fluid is much greater than unity, and bulbous end formation connected by a thin thread with several pinching necks when the conductivity ratio is much greater than unity. As the conductivity of the drop increases, the number of necks is decreased (Sherwood 1988). This may explain the distinctively different breakup modes observed in figures 3 to 6. However, these experimental data do not clarify whether the conductivity ratio is entirely responsible for this type of breakup, as suggested by Sherwood for the fluid pairs of identical viscosities.

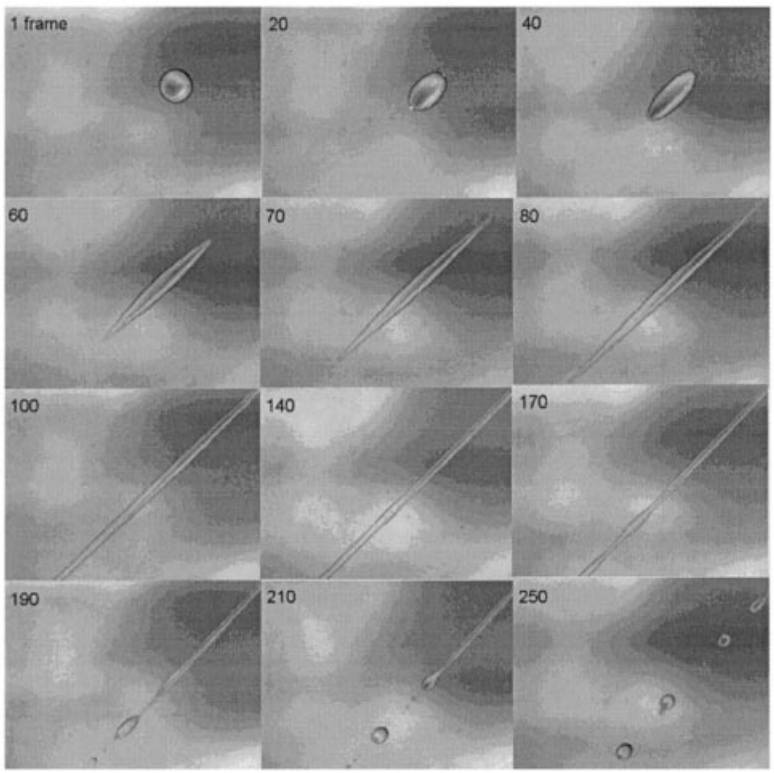

FIGURE 7. Breakup of a castor oil drop in silicone oil E (NN21 in table 1). The radius of the initial spherical drop is 0.16 cm and the applied electric field strength is 3.2 kV cm^{-1} ($\mathscr{E} = 1.1\mathscr{E}_c$). The frame rate is 15 frames s^{-1}.

Even for the breakup of a highly conducting drop, the reported results seem conflicting and/or inconclusive. In some investigations, highly conducting drops were broken up via tip streaming or pointed end formation. Moriya *et al.* investigated two classes of breakup mode depending on the dispersed-phase viscosity. Less viscous water droplets burst by tip streaming. However, they used a polymeric solution (30 wt% solution of polystyrene in di-*n*-butyl phthalate). As we shall see later, the deformation behaviour of a highly conducting drop can be significantly influenced by the non-Newtonian properties. Nishiwaki, Adachi & Kotaka (1988) also reported the breakup of highly conducting polypropylene oxide drops in polydimethylsiloxane with various viscosity ratios. Their results are consistent with ours. The breakup modes for less viscous drops and for more or comparably viscous drops are similar to figures 6 and 7, respectively.

4. Effect of non-Newtonian properties on the drop deformation and breakup

4.1. *Polymeric liquids used in this study*

In this section, we examine the deformation and breakup of polymeric liquid drops and discuss the effect of non-Newtonian properties from an electrohydrostatic point of view, which has been rigorously tested in the previous section. In doing this, the first step is to identify the parameters that are appropriate to characterize the fluids in an

Class	Abbreviation	Formulation	Viscosity (Pa s)
Elastic	PIB0	Mixture of polybutene and o-dichlorobenzene 7:3 by volume	1.586
	PIB1	0.5 wt% PIB solution in PIB0	2.307
	PIB2	1.0 wt% PIB solution in PIB0	2.617
	PAM1	1.5 wt% PAM solution in 0.1 M NaCl solution	0.485
	PAM2	2 wt% PAM solution in 0.1 M NaCl solution	3.018
	PAM3	3 wt% PAM solution in 0.1 M NaCl solution	11.840
Viscoelastic	XAN1	250 p.p.m. xanthan gun solution in XAN0	0.059
	XAN2	500 p.p.m. xanthan gum solution in XAN0	0.299
	XAN3	1000 p.p.m. xanthan gum solution in XAN0	0.658
	XAN4	2000 p.p.m. xanthan gum solution in XAN0	1.962
	XAN5	3000 p.p.m. xanthan gum solution in XAN0	7.087
	XAN6	4000 p.p.m. xanthan gum solution in XAN0	27.980

TABLE 3. Formulation and abbreviation of polymeric liquids used in the experiments. XAN0 stands for the mixture of deionized water and N, N-dimethylformaide.

electric-field-induced flow. For these experiments, we initially classified the polymeric liquids into two broad categories. One is purely elastic fluids, which exhibit an elastic fluid response such as normal stress differences in shear flow but an approximately shear-independent viscosity. Purely elastic fluids are often referred to as 'Boger fluids' or 'second-order fluids'. The other category is fully viscoelastic fluids, which exhibit both a shear-thinning viscosity and elasticity. It is often believed that we can draw some conclusions on the effects of elasticity and shear-thinning viscosity on the drop deformation and breakup problem simply from the fluid model classification. As we shall see later, however, this general characterization does not give much insight into the relationship between the observed drop behaviour and the fluid properties.

The non-Newtonian polymeric fluids used in these experiments are listed in table 3. The hydrophobic and leaky dielectric polyisobutylene (PIB) solutions were used as a continuous phase when the elastic properties of the medium were considered. PIB0 had shear viscosities independent of the shear rate and exhibited no significant normal stresses at a moderate shear rate, although it showed measurable normal stress at higher shear rates. On the other hand, both PIB1 and PIB2, which imitate a second-order fluid with shear-independent viscosity, exhibited considerable deviation from Newtonian behaviour. In figure 8(*a*), the shear viscosities and the first normal stress coefficients Π_1 of these solutions are plotted as a function of the shear rate. These solutions were prepared by the standard 'Boger fluid' preparation technique, i.e. dissolution of a small amount of high-molecular-weight polymer in a viscous solvent (Mackay & Boger 1987).

In order to examine the effect of non-Newtonian properties on the basis of the electrohydrostatic assumption, we prepared aqueous polymer solutions containing polyacrylamide (PAM, $M_w = 5 \times 10^6$ including 1.5 wt% acrylic acid, Aldrich) or xanthan gum (XAN, Aldrich) as the drop phase. Three purely elastic solutions were prepared by following the preparation method proposed by Tam & Tiu (1989): the small amount of high-molecular-weight PAM was dissolved in an aqueous 0.1M NaCl solution. The viscosities and the first normal stress difference coefficients for these fluids are plotted as a function of shear rate in figure 8(*b*) and their formulations are reported in table 3. The viscosities of these polymeric solutions remained relatively constant for shear rates less than about $1\,s^{-1}$. Xanthan gum solutions were used

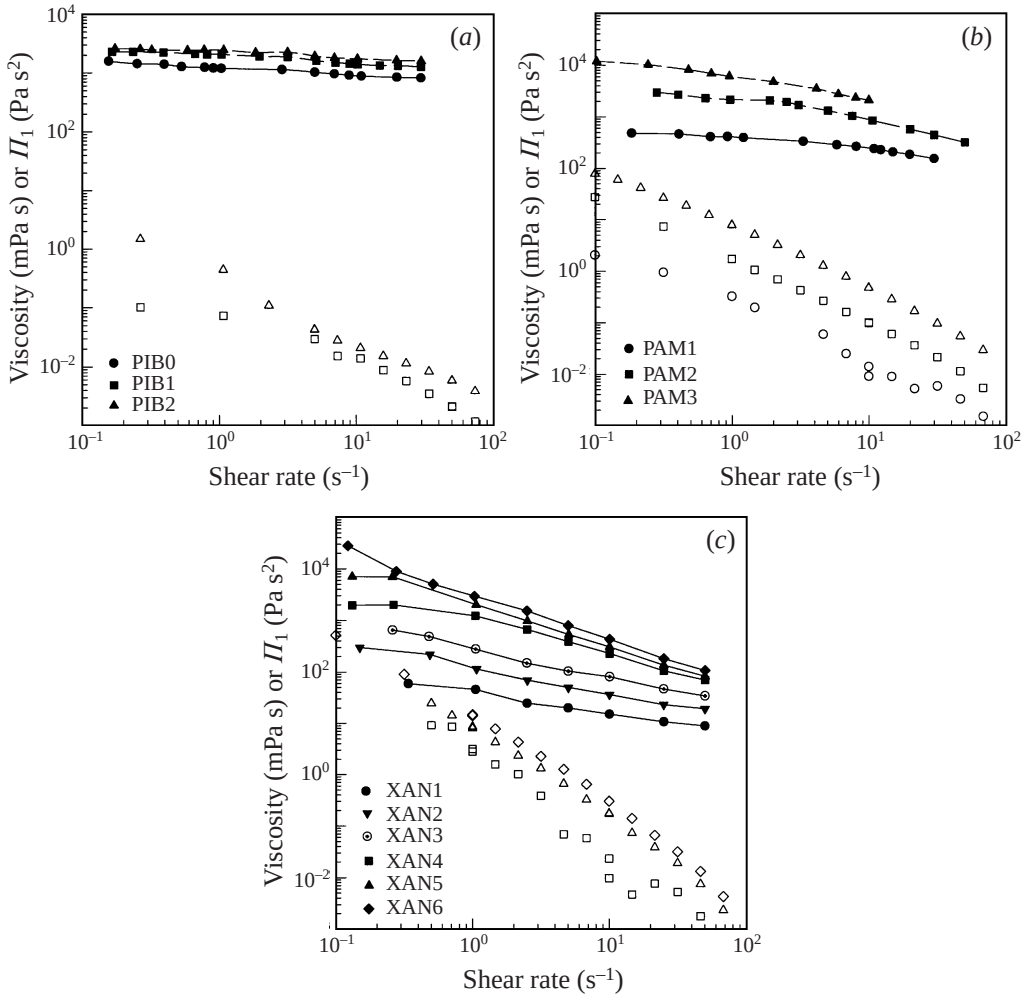

FIGURE 8. Shear viscosity (filled symbols) and the first normal stress coefficient (open symbols) of (*a*) elastic PIB solutions (the normal stress coefficient of PIB0 is not shown because it is too low to measure at low shear rates); (*b*) elastic PAM solutions; (*c*) viscoelastic XAN solutions (the normal stress coefficients of XAN1, XAN2, and XAN3 are too low to measure). For details see table 3.

in these experiments as fully viscoelastic fluids. These solutions exhibited significant shear-thinning viscosity. The shear viscosities and the first normal stress coefficients of xanthan gum solutions are shown in figure 8(*c*). Measurable normal stresses were found only in solution XAN4, XAN5, and XAN6.

4.2. *Deformation and breakup of polymeric liquid drops in a Newtonian fluid*

Now, let us begin by considering the deformations of purely elastic drops in a Newtonian fluid under the influence of a uniform electric field. The drop phases involved in these experiments showed elastic properties, but shear-independent viscosities as mentioned earlier. In addition, all of the drop phases considered in this section were highly conducting fluids and the resistivity ratio $R < O(10^{-5})$. In figure 9(*a*), the degree of drop deformation is illustrated as a function of the electric capillary number for these purely elastic drops. Also shown for comparison is the numerical solution

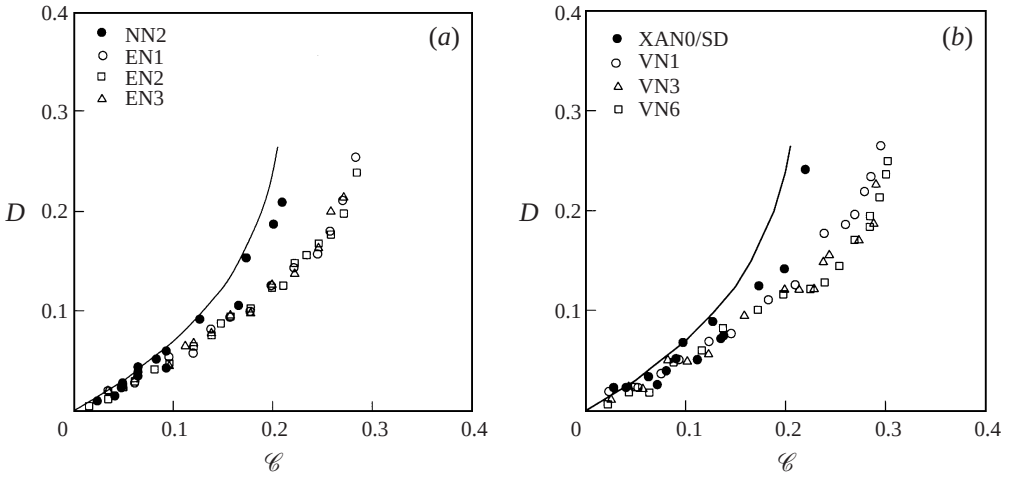

FIGURE 9. Degree of deformation of polymeric drops in silicone oil as a function of $\mathscr{C}$. (*a*) Elastic PAM drops; (*b*) viscoelastic XAN drops. The solid line represents the numerical prediction for a perfectly conducting drop calculated by Feng & Scott (1996) from the electrohydrostatic theory. See table 4 for details.

curve for a perfectly conducting drop. As noted, the degree of deformation of a highly conducting drop depends mainly on the electric capillary number. Obviously, the experimental results for the purely elastic and highly conducting drops agree well with the theory for the perfectly conducting drop only when the deformation is small. Indeed, the parameters other than the capillary number such as the drop-phase elasticity have no major influence on the drop deformation within the small deformation limit. However, as the drop deformation proceeds ($D > 0.1$), the deviation from the deformation behaviour of a highly conducting Newtonian drop becomes pronounced. For a given capillary number, the degree of deformation of the purely elastic drop is smaller than that of the purely viscous drop. As $\mathscr{C}$ increases, the numerical predictions for the perfectly conducting drop deviate considerably from the experimental results. Moreover, the critical capillary numbers of elastic drops are higher than that of the highly conducting Newtonian drop. These suggest clearly that the elastic properties of the drop phase suppress the drop deformation and tend to stabilize it.

Finally, the steady deformations of fully viscoelastic drops in a Newtonian medium are illustrated in figure 9(*b*). The deformation curves in this plot are for drops of three polymeric solutions (VN1, VN3, and VN6 in table 4) in silicone oil D. Also included for an illustrative purpose is the deformation curve of a Newtonian drop (XAN0) in silicone oil D. These four solutions have comparable electrical resistivities and permittivities but are highly conducting relative to the continuous phase. Although measured data are slightly scattered, the linear dependence of the degree of deformation on the electric capillary number is still preserved when the deformation is small. It can also be noted that the drop is stabilized by its viscoelasticity.

4.3. *Deformation and breakup of polymeric drops in a non-Newtonian fluid*

Let us turn to the steady deformation of Newtonian or non-Newtonian drops suspended in a non-Newtonian continuous phase in an electric field. The experimental runs are summarized in table 5. We begin with Newtonian drops immersed in elastic polyisobutylene solutions. The deformation behaviour can be found in figure 10(*a*). Clearly, the result of this experimental run NE1 is in good agreement with the numer-

Class	System	Drop Phase	Continuous phase	S	λ	Interfacial tension (N m^{-1})	Breakup mode
Elastic	EN1	PAM1	SD	26.6	0.417	0.0281	T
	EN2	PAM2	SD	26.6	2.5	0.0280	T
	EN3	PAM3	SD	26.6	10	0.0280	T
Viscoelastic	VN1	XAN1	SD	21.6	0.060	0.0146	N
	VN2	XAN2	SD	21.6	0.305	0.0142	N
	VN3	XAN3	SD	21.6	0.671	0.0134	T
	VN4	XAN4	SD	21.7	2.002	0.0137	T
	VN5	XAN5	SD	21.6	7.230	0.0139	T
	VN6	XAN6	SD	21.6	28.55	0.0155	T

TABLE 4. The list of experimental runs for the deformation and breakup of polymeric liquid drops suspended in Newtonian fluid. $R < 10^{-6}$. For the breakup modes, N and T stand for Newtonian-like breakup and tip streaming, respectively.

ical predictions for a highly conducting drop mentioned previously since the elasticity of PIB0 is negligible. The results included in figure 10(*a*) strongly indicate that the non-Newtonian properties, more specifically the elasticity of the continuous phase, stabilize the drop phase.

During the past decade, considerable efforts have focused on the breakup of viscoelastic drops in a Newtonian medium or Newtonian drops in a viscoelastic liquid which possesses both a non-Newtonian viscosity and appreciable elasticity. However, the effect of fluid elasticity was not understood completely for systems of viscoelastic fluids. Part of the problem arises from the fact that viscoelastic fluids may have both a non-Newtonian viscosity and elasticity, which may have a non-trivial effect on drop breakup. Milliken & Leal (1991) showed that the viscoelastic drops experienced deformation closely similar to that of Newtonian drops or were slightly stabilized for $\lambda > O(1)$. However, when $\lambda < O(1)$, the viscoelastic drops were significantly destabilized compared with the Newtonian drops. Evidently, at a certain viscosity ratio around unity, the elasticity of the drop phase reversed its effect from stabilizing to destabilizing the drop. According to Milliken & Leal and Varanasi, Ryan & Stroeve (1994), this occurs when the viscosity ratio lies between 0.1 and 1.

As illustrated in figure 10(*b*), when the viscosity ratio is around 0.2, the non-Newtonian properties of the two contiguous fluids do not play a major role in the drop deformation in our experiments. Although the continuous phase of PIB0 exhibits considerable normal stress differences at high shear rates, the normal stress differences for the drop phases in figure 10(*b*) are not large enough at low or moderate shear rates. As a consequence, the two phases are assumed to have negligible normal stress differences at low shear rates. It can be seen from figure 10(*b*) that elasticity of the continuous phase enhances the drop stability slightly. If the viscosity ratio is adjusted more carefully, the effect of viscoelasticity on the drop stability may be diminished. It is, thus, obvious that the results contained in figure 10(*b*) are consistent with the previous works on the stability of non-Newtonian fluid drops in a flow field.

In figure 10(*c*), the steady deformation is plotted versus the electric capillary number for purely elastic drops suspended in a non-Newtonian continuous phase. In these experimental runs, the viscosity ratios are slightly higher than unity. It is interesting to note that elasticity of the continuous phase destabilizes the non-Newtonian drop. For the case in which both the fluids are non-Newtonian, the controlling parameter in determining the drop stability is the ratio of the normal stress coefficients between the

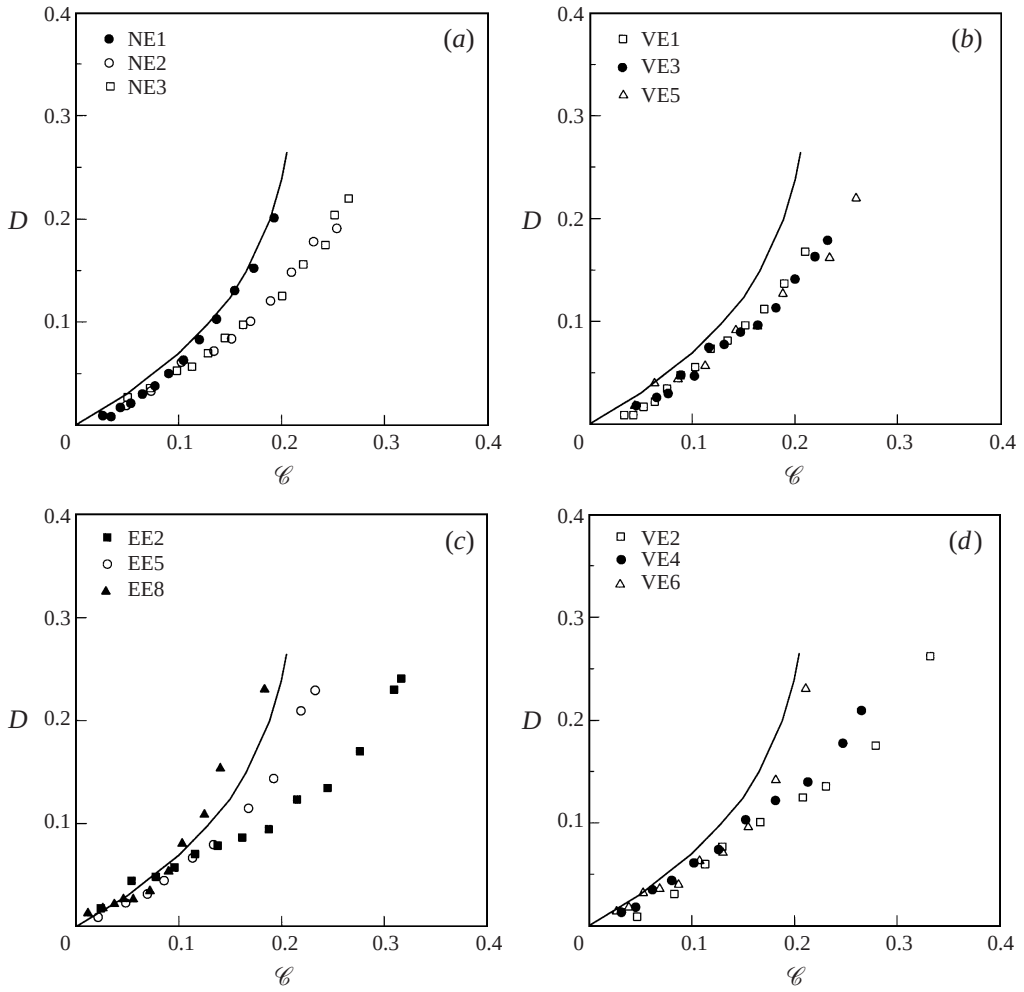

FIGURE 10. Degree of deformation of polymeric drops in elastic PIB as a functionc of $\mathscr{C}$. (*a*) XAN0 drops; (*b*) XAN2 drops; (*c*) PAM2 drops; (*d*) XAN6 drops. The solid line represents the numerical prediction for a perfectly conducting drop calculated by Feng & Scott (1996) from the electrohydrostatic theory. See table 5 for details.

drop and the continuous phases. As the ratio increases, the drop becomes more stable. In figure 10(*d*), the degree of deformation is plotted versus the capillary number for the viscoelastic drops in the purely elastic fluids. The deformation behaviour of the viscoelastic drops is quite similar to that of the elastic drops. In this case, thus, as the continuous phase has greater elasticity, the drop becomes less stable.

So far, we have investigated the steady deformation and the critical capillary number of polymeric liquid drops immersed in a Newtonian or non-Newtonian fluid. In summary, the stability of the drop is enhanced when either the drop or the continuous phase is non-Newtonian. Moreover, when both the drop and the continuous phase are non-Newtonian, the drop becomes more stable when the normal stress coefficient ratio increases. It is also found that when the viscosity ratio is larger than about 0.2, elasticity of the continuous phase destabilizes whereas the drop-phase elasticity stabilizes the drop. When the viscosity ratio is smaller than 0.2, the trend

Class	System	Drop phase	Continuous phase	S	λ	Interfacial tension ($N\,m^{-1}$)	Breakup mode
Newtonian	NE1	XAN0	PIB0	15.4	0.0005	0.0107	N
	NE2	XAN0	PIB1	15.4	0.0004	0.0109	N
	NE3	XAN0	PIB2	15.4	0.0003	0.0114	N
Elastic	EE1	PAM1	PIB0	19.0	0.33	0.0222	T
	EE2	PAM2	PIB0	19.0	2	0.0239	T
	EE3	PAM3	PIB0	19.0	8	0.0279	T
	EE4	PAM1	PIB1	19.0	0.23	0.0233	T
	EE5	PAM2	PIB1	19.0	1.364	0.0267	T
	EE6	PAM3	PIB1	19.0	5.46	0.0302	T
	EE7	PAM1	PIB2	19.0	0.185	0.0254	T
	EE8	PAM2	PIB2	19.0	1.11	0.0279	T
	EE9	PAM3	PIB2	19.0	4.44	0.0307	T
Viscoelastic	VE1	XAN2	PIB0	15.4	0.20	0.0109	N
	VE2	XAN6	PIB0	15.4	20	0.0099	T
	VE3	XAN2	PIB1	15.4	0.136	0.0126	T
	VE4	XAN6	PIB1	15.4	13.6	0.0181	T
	VE5	XAN2	PIB2	15.4	0.111	0.0130	T
	VE6	XAN6	PIB2	15.4	11.1	0.0212	T

TABLE 5. The list of experimental runs for the deformation and breakup of drops suspended in non-Newtonian fluid. $R < 10^{-5}$. For the breakup modes, N and T stand for Newtonian-like breakup and tip streaming, respectively.

is reversed. However, from the experimental observations reported here, it is found that the broad classification of polymeric solutions proposed in this study does not give much insight into the relationship between the observed drop behaviour and the fluid properties. This is because the electric-field-induced flow is weak, prior to the drop burst. As we shall see shortly, however, the non-Newtonian properties play a significant role during drop breakup in which large velocities and velocity gradients occur. This complicates the physics of modes of drop breakup and makes some results appear contradictory or confusing.

4.4. *Effect of non-Newtonian properties on the breakup mode*

When either the drop or the continuous phase is non-Newtonian, the drop exhibited distinctively different burst behaviour from that of Newtonian drops discussed in § 3. For illustration, microphotographs of the breakup of XAN6 drop in silicone oil D are reproduced in figure 11 for $\mathscr{C} = 1.1\mathscr{C}_c$. It can be clearly seen from figure 11 that the drops experienced tip steaming. The drop stretched slightly and the ends became sharply curved. As time proceeded, the ends became nearly pointed and then cusped. Immediately after the pointed ends were formed, a thin thread or small subdrops of fluid were ejected from the ends. The ends of the drop then retracted and the drop was restored to an ellipsoidal shape with pointed ends. Further increase in electric field strength induced the process of tip streaming again. Stretching of the drop to a large aspect ratio was not achieved. Throughout the process, fore-and-aft symmetry of the drop was not always maintained in our experiments. In many cases, tip streaming occurred only at one end of the drop. The droplets may lose their symmetrical shape because of traces of surface contaminants which inevitably lead to the non-homogeneity of interfacial properties (Ha & Yang 1995). In studies of hydrodynamic burst, Milliken & Leal (1991) suggested that in polymeric drops the nonlinearity of the

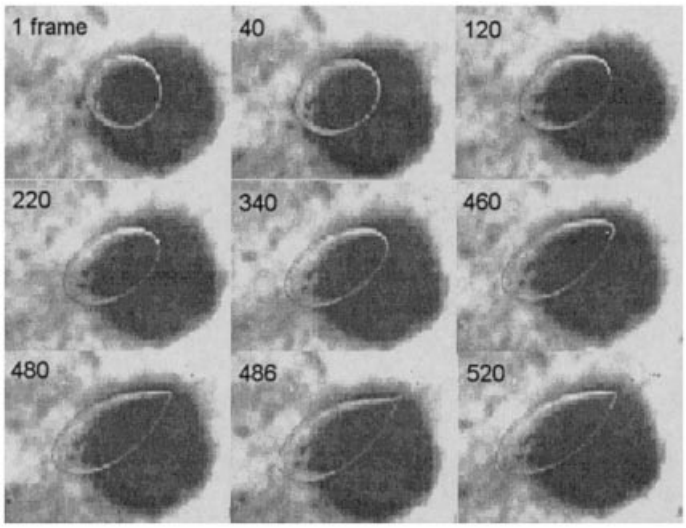

FIGURE 11. Microphotographs of tip streaming of an XAN6 drop in silicone oil D. The radius of the initial spherical drop is 0.27 cm and the applied electric field strength is 5.1 kV cm^{-1} ($\mathscr{E} = 1.1\mathscr{E}_c$). The frame rate is 15 frames s^{-1}.

stress–strain relationship renders the drop shape more sensitive to slight asymmetries in the flow field and that this causes the absence of fore-aft symmetry. This may be also true of the electric-field-induced burst of non-Newtonian drops.

Based on the results obtained for Newtonian-fluid pairs, it may be deduced that tip streaming observed in this study is caused by the non-Newtonian properties of the fluids. Also noted from comparison of experiments VN2 and VE3 (or VE5) is that the non-Newtonian properties of the continuous phase also induced tip streaming of a Newtonian drop. However, the mechanism is somewhat unclear to us. With regard to the tip streaming of polymeric liquid drops in an extensional flow field, Milliken & Leal (1991) suggested that the nonlinearity of the stress–strain relationship which rendered the drop shape more sensitive to slight asymmetries in the flow was responsible for the tip streaming. It has been also suggested that the tip streaming might be a consequence of the polymer molecules acting as amphiphilic low-molecular-weight surfactant molecules rather than being caused by some modification of the bulk rheology (Stone 1994). In substance, the water-soluble polymer used in this study acted like a surface-active agent. The addition of very small amount of polymer decreased the interfacial tension slightly. However, the effect of polymer molecules on the drop breakup mode is obviously different from that of low-molecular-weight surfactants. When the concentration of surfactant molecules was high enough, the breakup mode changed from tip streaming to the usual mode of a highly conducting Newtonian drop again. This phenomenon was observed in the experiments carried out in previous studies in an electric field (Ha & Yang 1998) and in a flow field (Bentley & Leal 1986; Stone & Leal 1989; de Bruijn 1993). Consequently, it can be concluded that the tip streaming results from the non-Newtonian properties of the constituent fluids, at least when the amount of dissolved polymer is considerable. Of course, in the case where a very small amount of polymer is dissolved, it may be reasonable to regard the polymer molecules as a surface-active agent since the non-Newtonian characteristics of the fluids are not so significant. This is especially true if the polymer molecules absorb on the interface.

5. Summary

In the present study, the deformation and breakup of Newtonian or non-Newtonian fluid drops in an external electric field have been studied. The continuous phase is either a Newtonian or non-Newtonian fluid. For Newtonian-fluid pairs, the electrohydrostatic assumption is valid when $R < O(10^{-5})$. Under this condition, the behaviour of a highly conducting drop agreed well with the numerical solution for a perfectly conducting drop in an insulating phase. Although the breakup mode of Newtonian drops is slightly influenced by the resistivity and viscosity ratios, R and λ, the overall features can be stated as follows. When the drop phase is highly conducting and much less viscous, the drop is fragmented via formation of bulbous ends and a thin waist. The appearance of bulbous ends shows that the highly viscous medium suppresses the formation of pointed ends. As the drop-phase conductivity decreases, the size of the bulb-like ends decreases and most of the drop volume remains in the mid-part. As the viscosity ratio increases up to $O(1)$, the shape of the drop ends becomes sharply pointed. In order to examine the effect of elasticity and shear-thinning viscosity separately, we classified the fluids into two broad categories: elastic and viscoelastic. It is found that the shear-rate dependence of viscosity is not effective in altering the behaviour of the drop phase. This is because the fluid motion induced by an electric field is too weak to induce a significant rheological response. The effect of non-Newtonian properties of the constituent fluids on the stability of highly conducting drops can be summarized as follows. When the viscosity ratio is larger than unity, elasticity of the drop phase enhances the drop stability. Equivalently, as the elasticity of the continuous phase increases, the drop becomes unstable. If the viscosity ratio is much smaller than unity, elasticity of the continuous phase produces stabilizing effects. The exchange from a stabilizing to destabilizing effect of the non-Newtonian continuous phase occurs when the viscosity ratio λ is around 0.2. In addition, the present experiments show that non-Newtonian properties of the fluids induce tip streaming. When both of two phases are non-Newtonian fluids, tip streaming is the prevalent mode of the drop breakup.

This work has been supported partly by the Ministry of Science and Technology and by a contracted research project with Hyundai Heavy Industries Co., Ltd. The authors appreciate their support.

REFERENCES

Ajayi, O. O. 1978 A note on Taylor's electrohydrodynamic theory. *Proc. R. Soc. Lond.* A **364**, 499–507.

Allan, R. S. & Mason, S. G. 1962 Particle behaviour in shear and electric fields. I. Deformation and burst of fluid drops. *Proc. R. Soc. Lond.* A **267**, 45–61.

Arp, P. A., Foister, R. T. & Mason, S. G. 1980 Some electrohydrodynamic effects in fluid dispersions. *Adv. Colloid Interface Sci.* **12**, 295–356.

Basaran, O. A. & Scriven, L. E. 1989 Axisymmetric shapes and stability of charged drops in an external electric field. *Phys. Fluids* A **1**, 799–809.

Basaran, O. A. & Wohlhuter, F. K. 1992 Effect of nonliner polarization on shapes and stability of pendent and sessile drops in an electric (magnetic) field. *J. Fluid Mech.* **244**, 1–16.

Baygents, J. C. & Saville, D. A. 1989 The circulation produced in a drop by an electric field: A high field strength electrokinetic model. In *Drops and Bubbles: Third Intl Colloq.* (ed. T. G. Wang), pp. 7–17. American Institute of Physics.

Beard, K. V., Ochs, H. T. & Kubesh, R. T. 1989 Natural oscillations of small raindrops. *Nature* **342**, 408–410.

Bentley, B. J. & Leal, L. G. 1986 An experimental investigation of drop deformation and breakup in steady, two-dimensional linear flows. *J. Fluid Mech.* **167**, 241–283.

Bird, R. B., Armstrong, R. C. & Hassager, O. 1987 *Dynamics of Polymeric Liquids*, 2nd edn. John Wiley.

Bruijn, R. A. de 1993 Tip streaming of drops in simple shear flows. *Chem. Engng Sci.* **48**, 277–284.

Cho, H. J., Kang, I. S., Kwoen, Y. C. & Kim, M. H. 1996 Study on the behavior of a bubble attached to the wall in a uniform electric field. *Intl J. Multiphase Flow* **22**, 909–922.

Chung, S. K. & Trinh, E. H. 1998 Containerless protein crystal growth in rotating levitated drops. *J. Cryst. Growth* **194**, 384–397.

Feng, J. Q. 1999 Electrohydrodynamics of a drop subjected to a steady uniform electric field at finite electric Reynolds number. *Proc. R. Soc. Lond.* A **455**, 2245–2269.

Feng, J. Q. & Scott, T. C. 1996 A computation analysis of electrohydrodynamics of a leaky dielectric drop in an electric field. *J. Fluid Mech.* **311**, 289–326.

Garton, C. G. & Krasucki, Z. 1964 Bubbles in insulating liquids: stability in an electric field. *Proc. R. Soc. Lond.* A **280**, 211–226.

Ha, J.-W. 1999 Deformation and breakup of emulsion drops in an electric field. PhD thesis, Korea Advanced Institute of Science and Technology.

Ha, J.-W. & Yang, S.-M. 1995 Effects of surfactant on the deformation and stability of a drop in a viscous fluid in an electric field. *J. Colloid Interface Sci.* **175**, 369–385.

Ha, J.-W. & Yang, S.-M. 1998 Effects of non-ionic surfactant on the deformation and stability of a drop in an electric field. *J. Colloid Interface Sci.* **206**, 195–204.

Ha, J.-W. & Yang, S.-M. 1999*a* Fluid dynamics of a double emulsion droplet in an electric field. *Phys. Fluids*, **11**, 1029–1041.

Ha, J.-W. & Yang, S.-M. 1999*b* Breakup of multiple emulsion drops in a uniform electric field. *J. Colloid Interface Sci.* **213**, 92–100.

Ha, J.-W. & Yang, S.-M. 1999*c* Rheological responses of oil-in-oil emulsions in an electric field. *J. Rheol.* (accepted for publication).

Ha, J.-W. & Yang, S.-M. 1999*d* Electrohydrodynamics and electrorotation of a deformable conducting drop in a more conducting fluid. *Phys. Fluids* (accepted for publication).

Kang, I. S. 1993 Dynamics of a conducting drop in a time-periodic electric field. *J. Fluid Mech.* **257**, 229–264.

Mackay, M. E. & Boger, D. V. 1987 An explanation of the rheological properties of Boger fluids. *J. Non-Newtonian Fluid Mech.* **22**, 235–243.

Marszalek, P. & Tsong, T. Y. 1995 Cell fission and formation of mini cell bodies by high frequency alternating electric field. *Biophys. J.* **68**, 1218–1221.

Melcher, J. R. & Taylor, G. I. 1969 Electrohydrodynamics: a review of the role of interfacial shear stresses. *Ann. Rev. Fluid Mech.* **1**, 111–146.

Miksis, M. J. 1981 Shape of a drop in an electric field. *Phys. Fluids* **24**, 1967–1972.

Milliken, W. J. & Leal, L. G. 1991 Deformation and breakup of viscoelastic drops in planar extensional flows. *J. Non-Newtonian Fluid Mech.* **40**, 355–379.

Moriya, S., Adachi, K. & Kotaka, T. 1986 Deformation of droplets suspended in viscous media in an electric field: I. Rate of deformation, II. Burst behaviour. *Langmuir* **2**, 155–165.

Nishiwaki, T., Adachi, K. & Kotaka, T. 1988 Deformation of viscous droplets in an electric field: Poly(propylene oxide)/poly(dimethylsiloxane) systems. *Langmuir* **4**, 170–175.

O'Konski, C. T. & Harris, F. E. 1957 Electric free energy and the deformation of droplets in electrically conducting systems. *J. Phys. Chem.* **61**, 1172–1174.

O'Konski, C. T. & Thacher, H. C. 1953 The distortion of aerosol droplets by an electric field. *J. Phys. Chem.* **57**, 955–958.

Pan, X.-D. & McKinley, G. H. 1997 Characteristics of electrorheological responses in an emulsion system. *J. Colloid Interface Sci.* **195**, 101–113.

Ptasinski, K. J. & Kerkhof, P. J. A. M. 1992 Electric field driven separations: Phenomena and applications. *Sep. Sci. Technol.* **27**, 995–1021.

Rhim, W. K., Chung, S. K., Hyson, M. T., Trinh, E. H. & Elleman, D. D. 1987 Large charged drop levitation against gravity. *IEEE Trans. Ind. Appl.* **IA-23**, 975–979.

Sartor, J. D. 1969 Electricity and rain. *Phys. Today* **22**, August, 45–51.

Saville, D. A. 1997 Electrohydrodynamics: The Taylor–Melcher leaky dielectric model. *Ann. Rev. Fluid Mech.* **29**, 27–64.

Scott, T. C. 1989 Use of electric fields in solvent extraction: A review and prospect. *Sep. Purif. Methods* **18**, 65–109.

Sherwood, J. D. 1988 Break-up of fluid droplets in electric and magnetic fields. *J. Fluid Mech.* **188**, 133–146.

Stone, H. A. 1994 Dynamics of drop deformation and breakup in viscous fluids. *Ann. Rev. Fluid Mech.* **26**, 65–102.

Stone, H. A. & Leal, L. G. 1989 A note concerning drop deformation and breakup in biaxial extensional flows at low Reynolds numbers. *J. Colloid Interface Sci.* **133**, 340–347.

Stone, H. A., Lister, J. R. & Brenner M. P. 1999 Drops with conical ends in electric and magnetic fields. *Proc. R. Soc. Lond.* A **455**, 329–347.

Tajiri, K., Ohta, K., Nagaya, T., Orihara, H., Ishibashi, Y., Doi, M. & Inoue, A 1997 Electrorheological effect in immiscible polymer blends. *J. Rheol.* **41**, 335–341.

Tam, K. C. & Tiu, C. 1989 A low viscosity, highly elastic ideal fluid. *J. Non-Newtonian Fluid Mech.* **31**, 163–177.

Taylor, G. I. 1964 Disintegration of water drops in an electric field. *Proc. R. Soc. Lond.* A **280**, 383–397.

Taylor, G. I. 1966 Studies in electrohydrodynamics. I. The circulation produced in a drop by an electric field. *Proc. R. Soc. Lond.* A **291**, 159–166.

Torza, S., Cox, R. G. & Mason, S. G. 1971 Electrohydrodynamic deformation and burst of liquid drops. *Phil. Trans. R. Soc. Lond.* **269**, 259–319.

Varanasi, P. P., Ryan, M. E. & Stroeve, P. 1994 Experimental study on the breakup of model viscoelastic drops in uniform shear flow. *Ind. Engng Chem. Res.* **33**, 1858–1866.

Venugopal, G. & Krause, S. 1992 Development of phase morphologies of poly(methylmethacrylate)-polystyrene-toluene mixtures in electric fields. *Macromolecules* **25**, 4626–4634.

Venugopal, G., Krause, S. & Wnek, G. E. 1989 Modification of polymer blend morphology using electric fields. *J. Polymer Sci.* C: *Polymer Lett.* **27**, 497–501.

Vizika, O. & Saville, D. A. 1992 The electrohydrodynamic deformation of drops suspended in liquids in steady and oscillatory electric fields. *J. Fluid Mech.* **239**, 1–21.

Winterhalter, M., Klotz, K.-H., Benz, R. & Arnold, W. M. 1996 On the dynamics of the electric field induced breakdown in lipid membranes. *IEEE Trans. Ind. Appl.* **32** 125–130.

Wohlhuter, F. K. & Basaran, O. A. 1992 Shapes and stability of pendent and sessile dielectric drops in an electric field. *J. Fluid Mech.* **235**, 481–510.

Xi, K. & Krause, S. 1998 Droplet deformation and structure formation in two-phase polymer/polymer/toluene mixtures in an electric field. *Macromolecules* **31**, 3974–3984.